Experimental Study on Ice Shear Strength Evolution

Gong Chen, Weiling Kong, and Fuxin Wang

Abstract Prediction of ice shearing performance on aluminum substrate is significant to develop de-icing technology for engineering problems. Ice shearing stress, which involves both adhesion and cohesion, varies with progression of substrate-icing both in temporal and spatial. Thus, study on evolution of both during substrate icing helps comprehensive understanding regularity of shearing performance. In this research, an experiment is designed to measure both ice adhesive and cohesive strength. Afterward, the evolutionary law is discussed with both physical and thermal theories. Experiment results show that substrate icing could be divided into several stage in sequence as "freezing", "cooling" and "equilibrium". Both adhesive and cohesive strength increases obviously in the freezing and cooling stage, while finally converges in the equilibrium stage. Such evolution of ice adhesive and cohesive strength are contribute to gradual change of temperature during vertical growing of ice layer. Finally, A model is established to evaluate the adhesive and cohesive strength via given initial temperature, time and position.

Keywords Substrate-icing · Ice adhesive strength · Thermal diffusion

1 Introduction

Ice shedding is a common physical phenomenon which bring serious engineering problems, especially in the field of aviation and aerospace. For instance, ice cube shed from aircraft surface might be sucked into the air-turbo-engine and causes damage to engine component [1]. Also, irregular geometric configuration of turbo-blade front edge after ice shedding might result in aerodynamics deterioration.

G. Chen · W. Kong (✉) · F. Wang
School of Aeronautic and Astronautic, Shanghai Jiao Tong University, Shanghai, China
e-mail: kongwl@sjtu.com

G. Chen
Department of Advanced Vehicle Development and Vehicle Integration, Pan-Asia Technical Automotive Center Co, Ltd., Shanghai, China

Z. Jing and X. Zhan (eds.), *Proceedings of the International Conference on Aerospace System Science and Engineering 2020*, Lecture Notes in Electrical Engineering 680,
https://doi.org/10.1007/978-981-33-6060-0_6

In essences, ice shedding happens as long as external load, such as aerodynamics load, centrifugal inertial force, or even gravity, exceed its attaching force to substrate. Such attaching force could be either "adhesion" or "cohesion" according to their mechanism. Ice adhesion is defined as the molecular force on the interface between ice and substrate. In contrast, ice cohesion is defined as the inter-molecular force of ice. Ice adhesion and cohesion could be either shearing or normal. In most case, shearing performance is more focused in ice shedding problem.

It has been found that both adhesion and cohesion are influenced by many factors according to the research in recent years. Kraj [2], Zou [3], Kulinich [4] find ice adhesion is sensitive to physical and chemical properties of substrate surface. Ice adhesion to substrate ranges from 0.05Mpa to 0.5Mpa with different surface roughness and coating treatment. Jellinek [5], Guerin [6], Janjua [7] and Archer [8] find that both ice adhesive and cohesive strength are temperature-dependent. Chu [9] also points out adhesion and cohesion also related to the geometry and configuration of the water before freezing.

However, In most of the literatures above, both ice adhesion and cohesion are regarded as steady state parameters after complete substrate-icing. There is few attention has been paid on the evolution of ice adhesion and cohesion during ice progression. However, in reality, adhesion or cohesion failure usually occurs before complete ice formation. For instance, larger aerodynamic load leads to ice shedding or breaking from the front edge of airfoil as soon as ice is partly accumulated. Also, ice shedding usually occurs with a little residual ice remains on the surface of aircraft fuselage. Thus, temporal and spatial evolution during freezing deserves more study for comprehensive prediction and effective prevention of ice shedding.

In this research, experiment is designed to measure the both ice adhesive strength and cohesive strength at each significant moment within a substrate icing process. Afterward, both mechanical and thermal effect are discussed respectively to find the main cause of the experimental results. Finally, a analytical model is established for qualitative description of such evolutionary law.

2 Research Method

2.1 Experiment Apparatus and Strategy

The arrangement of experimental apparatus is shown in Fig. 1. It includes three main part: cooling box, icing specimen and force measuring system. The cooling box is filled with glycol ethylene as the coolant for temperature controlling by an external refrigerator with bump. An icing specimen is located in the space inside cooling box. The specimen is composed by a basement and a slider. A thermal couple is embedded into the slider for monitoring temperature while a electric vibrator is attached on the basement for icing-triggering. The horizontal translation of the slider inside groove

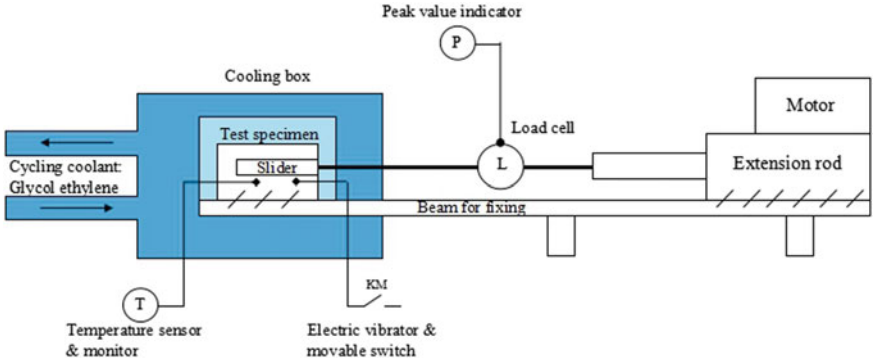

Fig. 1 Arrangement of experiment apparatus

is achieved by an electric extendable rod. Between slider and the rod, a load cell is installed for measuring the load.

The structure and function of the icing specimen is shown in Fig. 2. Both of the basement and slider are made of 6061 aluminium, which is widely used in aviation engineering. The slider, on which there is groove, is inserted in the tunnel of the basement. Vaseline is coated in clearance between basement and slider for sealing, lubrication and preventing unexpected freezing. The ultra-purred water used in experiment is prepared by a purifier (RS2200QUV, Rephile Bioscience, Ltd) in order to satisfy the laboratory standard. The water is filled in the cuboid hollow composed of the slider and basement. The length l and width w of the hollow cross section are 10 mm and 12 mm respectively while the depth d of the hollow is variable.

As shown in Fig. 2, icing is triggered by switching on the vibrator at particular temperature. An increasing load F is applied on the slider in horizontal direction to pull out the slider until displacement occurs. The payload is recorded by the peak value indicator.

As shown in Fig. 3, force-measurement on section planes with different distance to substrate is achieved by alternating a group of individual slider with different deep hollow. Slider with no hollow (d_0) is applicable for measurement of adhesive strength between ice and substrate. While for cohesive strength measurement, the distance of the tested section to substrate is numerically equal to the depth, d, of slider hollow.

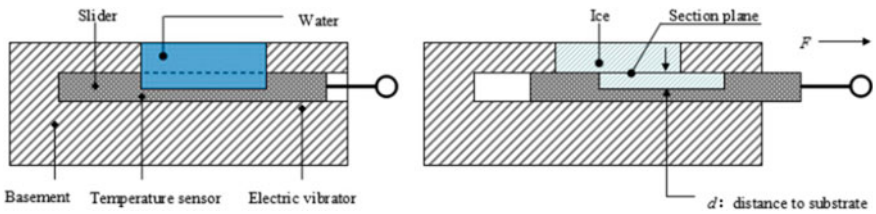

Fig. 2 Structure and principle of the ice specimen

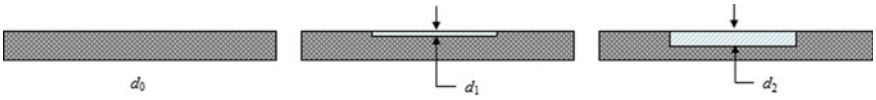

Fig. 3 Slider for measurement on different section plane

The shear stress F_τ of ice on the section is numerically equal to the payload F when the displacement occurs. The shear strength τ is then calculated with section plane area A of the hollow.

$$F_\tau = F \tag{1}$$

$$\begin{cases} \tau = \dfrac{F_\tau}{A} = \begin{cases} \tau_{\text{adheison}}(\tau_{ad}) & (d = 0) \\ \tau_{\text{coheison}}(\tau_{co}) & (d \neq 0) \end{cases} \end{cases} \tag{2}$$

Measurement of adhesive strength τ_{ad} or cohesion strength τ_{co} on different distant sections is alternated easily by changing different slider.

2.2 Experiment Condition and Variables

As mentioned above, evolution of either adhesive or cohesive strength happens in both spatial or temporal, and it also sensitive to ambient temperature. Therefore, three variables are involved in this experiment: freezing time t, distance from shear section to substrate d and initial ambient temperature T.

Freezing time, t

Five moments are followed for the same experiment condition to reflect status at each icing stage. The specific selection of moment is shown in Sect. 3.1.

Position of shear section, d

Three sections with different short distance d: $d_0 = 0$ mm, $d_1 = 1$ mm, $d_2 = 2$ mm is selected to identify the spatial evolutionary trend of shearing performance.

Initial temperature, T_∞

Effect of temperature is always concerned for all the icing problem. For substrate-icing, ice shearing performance is still changeable and unclear within the temperature range of [271.15, 267.15 K] in previous study by our colleague [10]. Thus, $T_\infty = 27.015$ K and $T_\infty = 267.65$ K are selected as the two variables for the experiment. For better illumination, relative initial temperature to equilibrium freezing point $\Delta T_\infty (\Delta T_\infty = |T_\infty - T_m|)$ is also used besides absolute value in following discussion.

3 Experiment Results

3.1 Changing History of Substrate Temperature

Before shearing stress measurement, temperature near substrate is monitored every minute for tracing its changing history during substrate-icing process. Two temperature history curves, which are corresponding to the two initial temperature $T_{\infty 1} = 27.015$ K and $T_{\infty 2} = 267.65$ K, are plotted in Fig. 4. Each curve is numerically fitted by averaging the values from at least four repeated attempts.

The result shows the temperature history of the two conditions are qualitatively similar. Both curves of $\Delta T(t)$ are in accord with the freezing principle of supercooled water [6]. According to feature of the curves, the progression of substrate-icing could be divided into four stages.

Stage 0: Triggering. As soon as external impulse is applied on the ice specimen, icing is immediately triggered from the substrate surface and the temperature suddenly re-calescence to the equilibrium freezing point. This stage usually lasts less than 1 s so that it could be regarded as instantaneous.

Stage I: Freezing. Phase transition of water from liquid to solid occurs right after sudden temperature re-calescence. Latent heat due to continuous phase transition releases from the substrate so that freezing field almost remains at equilibrium freezing point T_m. This process lasts until the phase transition is absolutely accomplished.

Stage II: Cooling. Phase transition is absolutely completed and no latent heat released anymore. Then, ice domain is cooled continuously until it reaches to initial temperature T_∞.

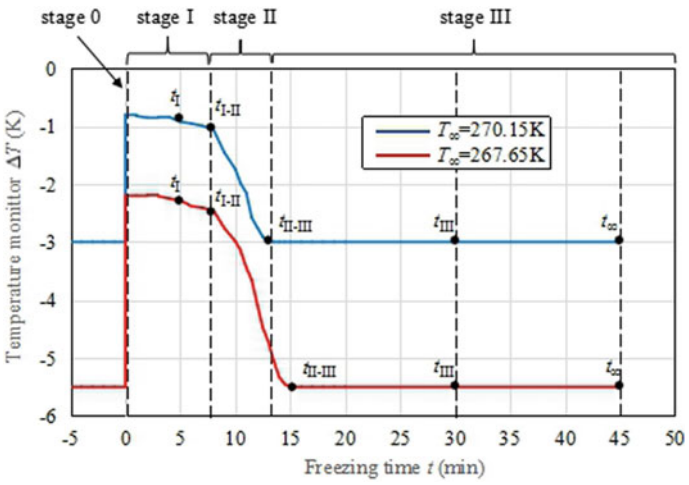

Fig. 4 Temperature history monitored from substrate

Table 1 Time duration of each icing stage

T_∞(K)	Stage I	Stage II	Stage III
270.15	[0.0, 8.0 min]	[8.0, 13.5 min]	[13.5 min,∞]
267.65	[0.0, 8.0 min]	[8.0, 15.0 min]	[15.0 min,∞]

Table 2 Time point for ice adhesion/cohesion measurement

T_∞(K)	t_{I}	$t_{\mathrm{I–II}}$	$t_{\mathrm{II–III}}$	t_{III}	t_∞
270.15	≈3 min	≈8.0 min	13.5 min	30 min	45 min
267.65	≈3 min	≈8.0 min	15.0 min	30 min	45 min

Stage III: Equilibrium. No more energy conversion and heat conduction occurs so that thermodynamic equilibrium is achieved.

It is notable that freezing stage and cooling stage are divided here for better illumination of substrate-icing progression. In reality, however, these stages usually process simultaneously without any clear boundary. It means the cooling of the ice layer occurs as soon as it is formed from supercooled water under the effect of substrate-heat conduction.

Time duration of each icing stage is listed in Table 1. It shows that they are slightly different with the conditions of two initial temperature. Icing in the condition with lower initial temperature requires a bit longer time for finishing stage II and III.

As marked in Fig. 4 as well as listed in Table 2, t_{I}, $t_{\mathrm{I–II}}$, $t_{\mathrm{II–III}}$, t_{III}, t_∞ are set as "critical icing moment" for force measurement. $t_{\mathrm{I–II}}$ and $t_{\mathrm{II–III}}$ are the transition moment from stage I to stage II and from stage II to stage III. While t_{I} and t_{III} are the interpolated moment for stage I and stage III. t_∞ is the moment that stage III lasts for enough time. Measurements are made at these five moment to trace the evolution.

3.2 *Results of Ice Adhesive Strength, τ_{ad}*

Measurements of adhesive strength τ_{ad} are made at each of the five critical moments of both two temperature conditions. The results are illustrated in Fig. 5a, b respectively.

According to the result in each figure, it is noticeable that τ_{ad} increases gradually in stage I and stage II while such increment reduces in following period and finally tend to convergent at the end of stage III. Comparing to the result in both of the two figure, it is also notable that the final converged value of τ_{ad} when $T_\infty = 267.65\,\mathrm{K}$ is slightly higher than that when $T_\infty = 270.15\,\mathrm{K}$.

Table 3 listed the statistical data of adhesion as the supplement to that in Fig. 5. It is obvious that large dispersion of measurement occurs at first moment and then reduces for the rest. Such status indicates that ice-adhesion is unstable at the early stage of icing while it tend to be stable in the end.

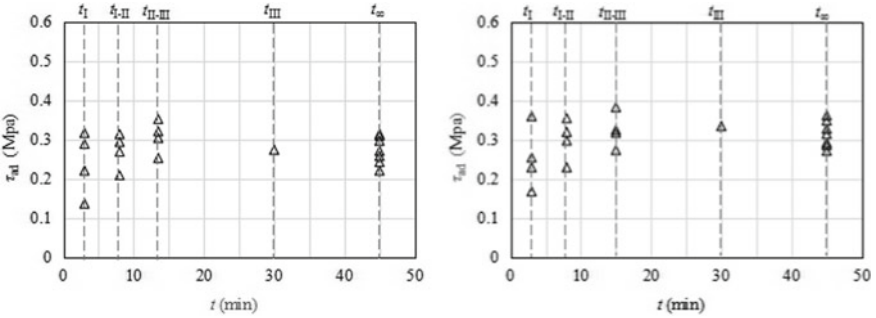

(a) T_∞=270.15K **(b) T_∞=267.65K**

Fig. 5 Evolution of ice adhesion during substrate icing

Table 3 Statistical data of adhesion measurement (Mpa)

T_∞(K)	t_I		$t_{I–II}$		$t_{II–III}$		t_{III}		t_∞	
	Mean	Stdv	Mean	Stdv	Mean	Stdv	Mean	Stdv	Mean	Stdv
270.15	0.241	0.080	0.272	0.045	0.308	0.041	0.274	/	0.273	0.035
267.65	0.252	0.081	0.299	0.052	0.324	0.045	0.334	/	0.314	0.029

3.3 *Results of Ice Cohesive Strength, τ_{co}*

Measurements of cohesive strength τ_{co} are made at each of the five critical moments of both two temperature conditions at the two certain sections. The results are illustrated in Fig. 6a–d respectively.

As shown in Fig. 6a, b, the evolutionary trend of cohesive strength at the closer section is illustrated. Tremendous increasing of τ_{co} is observed during stage I and stage II, which is dramatically larger than that of ice adhesion at same period as that in Fig. 5a, b. In stage III, cohesive strength is converged gradually, of which the value is negatively related to initial temperature $\boldsymbol{\Delta T_\infty}$.

As shown in Fig. 6c, d, the situation of cohesive strength at a more distant section is similar to that in Fig. 6a, b. The only difference is that the value at moment t_I is extremely low, some of which is even lower than the minimum sensitivity of the instrument. In fact, the measurement of cohesive strength is not always available at such early moment. Only about one-fourth attempts are able to produce effective results.

The statistic data in Table 4 reflects numerical characteristics of cohesion. Compare to that of adhesion in Table 3, the increasing trend of cohesion at the given two sections is much more obvious. In addition, it is similar that lower initial temperature leads to higher convergent value of cohesion at the end of substrate icing progression. It is also noteworthy that, especially in stage I and II, the cohesive strength at a closer section to substrate is lightly larger than that at a more distant. Such status is diminished in stage III.

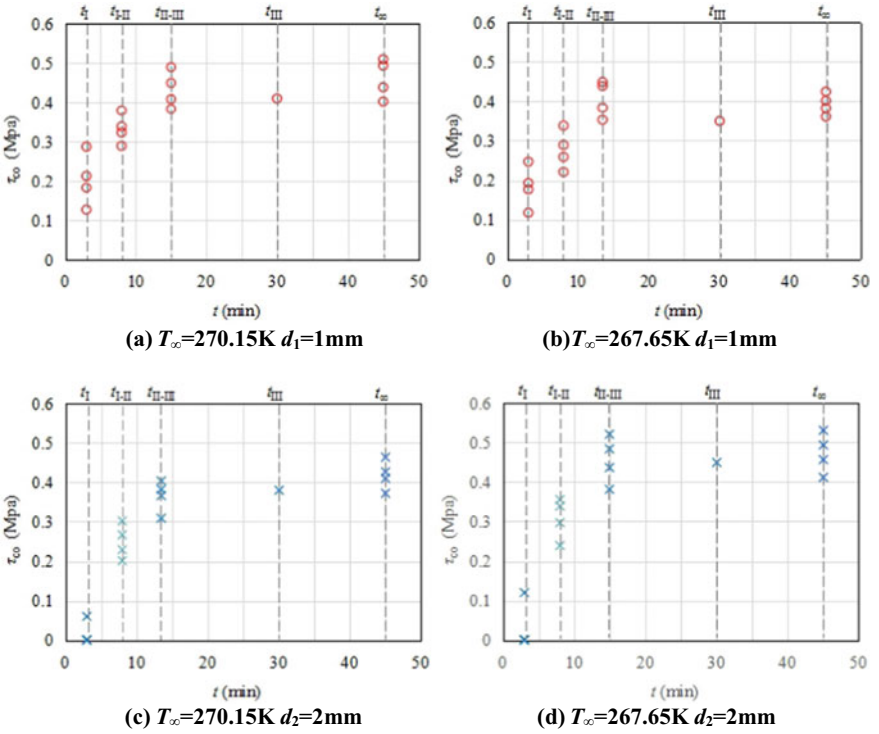

(a) T_∞**=270.15K** d_1**=1mm** **(b)**T_∞**=267.65K** d_1**=1mm**

(c) T_∞**=270.15K** d_2**=2mm** **(d)** T_∞**=267.65K** d_2**=2mm**

Fig. 6 Evolution of ice cohesion during substrate icing

Table 4 Statistical data of cohesion measurement (Mpa)

T_∞(K)	t_I		$t_{I–II}$		$t_{II–III}$		t_{III}		t_∞	
$d_1 = 1$ mm										
	Mean	Stdv	Mean	Stdv	Mean	Stdv	Mean	Stdv	Mean	Stdv
270.15	0.183	0.054	0.276	0.049	0.406	0.046	0350	/	0.392	0.027
267.65	0.206	0.067	0.332	0.037	0.432	0.046	0.409	/	0.461	0.049
$d_2 = 2$ mm										
	Mean	Stdv	Mean	Stdv	Mean	Stdv	Mean	Stdv	Mean	Stdv
270.15	/	/	0.249	0.044	0.365	0.041	0.379	/	0.419	0.038
267.65	/	/	0.308	0.052	0.456	0.060	0.449	/	0.473	0.051

3.4 Summary of Experiment Results

The general evolutionary trend of both ice adhesion and cohesion in each stage during substrate icing could be summarized according to the experiment result in 3.2 and 3.3 respectively as follow:

(1) Both adhesion and cohesion increase during the substrate icing progression. Both of the increment are large in stage I and stage II, and then they reduce in stage III and final converge at the end of the icing process.

$$\text{Stage I\&II}: \begin{cases} \tau_{ad}(t_1) < \tau_{ad}(t_2) \\ \tau_{co}(t_1) < \tau_{co}(t_2) \end{cases} \quad 0 < t_1 < t_2 < t_{\text{II–III}} \tag{3}$$

$$\text{Stage III}: \begin{cases} \lim\limits_{t\to\infty} \tau_{ad}(t) = [\tau_{ad}] \\ \lim\limits_{t\to\infty} \tau_{co}(t) = [\tau_{co}] \end{cases} \quad t_{\text{II–III}} < t < \infty \tag{4}$$

(2) The final converged value of both adhesion and cohesion at the end of icing process are negatively relative to initial temperature.

$$\begin{cases} [\tau_{ad}(T_1)] < [\tau_{ad}(T_2)] \\ [\tau_{co}(T_1)] < [\tau_{co}(T_2)] \end{cases} \quad (T_1 > T_2) \tag{5}$$

(3) With the condition of the same initial temperature, ice adhesive strength is numerically different to cohesive strength. In general, the final converged value of cohesive strength is usually larger than that of the adhesive strength.

$$[\tau_{ad}(T_1)] < [\tau_{co}(T_1)] \tag{6}$$

(4) Evolution of ice cohesion has been identified in spatial. It is earlier for ice cohesion to generate and develop at a closer section to substrate while there is a delay in time for such generation and development at a more distant section. With the icing progression, cohesion at different section tend to be uniform at last.

$$\begin{cases} \tau_{co}(d_1) < \tau_{co}(d_2) \\ \lim\limits_{t\to\infty} [\tau_{co}(d_1) - \tau_{co}(d_2)] \to 0 \end{cases} \quad (d_1 > d_2) \tag{7}$$

In summary, we find a gradually-convergent increasing trend of both ice adhesion and cohesion in temporal and spatial. And such evolution is strongly related to substrate icing progression.

4 Evolution of Thermal Condition During Substrate Icing

It has been summarized in Sect. 3.4 that evolution of ice adhesion and cohesion is coupled with substrate-icing. Moreover, according to the results obtained from previous research of our group [11, 12], thermal condition, especially the transient local temperature of on growing ice layer, changes continuously. Since temperature is regarded as the significant factor which affect both ice adhesion and cohesion

as mentioned in the introduction, it is necessary to focus the law and principle of temperature variation during substrate icing progression.

4.1 Principle of Thermal Condition During Substrate Icing

Referring to the monitored temperature changing history in Sect. 3.1, a simplified illustration is assumed to describe thermal condition during a substrate icing. As shown in Fig. 7, a "finite element" is introduced to illustrate thermal status of ice formation near the substrate.

Firstly, before ice growing, the entire finite element, which includes both supercooled water and substrate surface, remains at equilibrium freezing point T_{m}.

Afterward, phase transition from liquid to solid begins as soon as ice being triggered. Ice layer grows continuously in vertical direction, which represents upward moving of the ice-water interface. Simultaneously, the temperature of the frozen ice layer is gradually cooling down from equilibrium freezing point T_m to initial temperature T_∞ again due to the high heat conductivity of the aluminium substrate.

Finally, since substrate icing is entirely complete and temperature difference between substrate and ice layer is absolutely eliminated, neither latent heat dissipation nor heat conduction occurs so that the system tends to equilibrium.

In summary, temperature variation mainly occurs during the vertical growth of ice layer. Hence, analytical solution of dynamic temperature field should be considered with relevant icing principles.

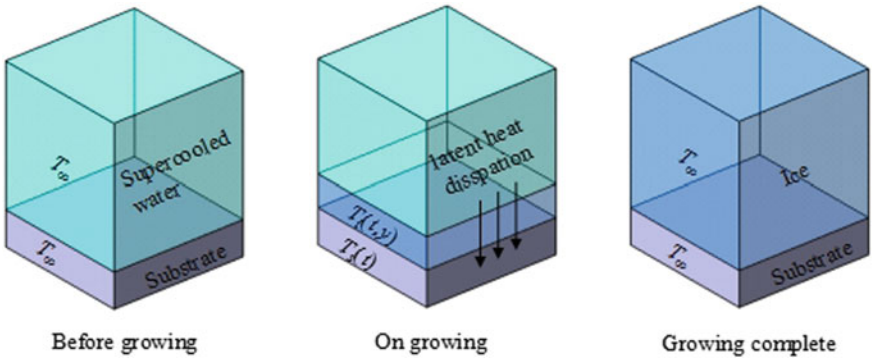

Fig. 7 Thermal status of "finite element" during substrate icing

4.2 Analytical Solution of Temperature Field

Usually, "unsteady state heat transfer theory" is commonly used to solve the problem of temperature variation within different media. The system, which is composed of substrate and supercooled water or ice could be treated as "semi infinite body" and the time/position-dependent temperature field $T_i(t, y)$ is consequently derived by the unsteady state heat transfer equation as shown (8).

$$\frac{\partial T_i}{dt} - a_i \frac{\partial^2 T_i}{dy^2} = 0 \quad 0 < y < h_i(t) \tag{8}$$

In which a_i is the diffusive coefficient of ice. t and y are the time and position dependent variable of the temperature filed. *hi(t)* is the dynamic range of temperature field, which is physically equal to transient thickness of on growing ice layer. Generally speaking, compared to the aluminium substrate, ice is not an effective heat conductor due to its lower heat conductivity. In this situation, temperature gradient within the range of on growing ice layer is reasonable to simplified as linear. Hence, transient local temperature $T(t, y)$ within the ice layer could be analytically solved with two available boundary condition of temperature. They are the temperature of ice-water interface $T_{i-w}(t)$ and the temperature of substrate-ice interface, $T_{i-s}(t)$.

$$T = \begin{cases} T_{i-w}(t, y) & y = h_i \\ T_{i-s}(t, y) & y = 0 \end{cases} \tag{9}$$

In addition, the range of linear temperature gradient is also need be considered as a time-dependent function.

$$y = h_i = h_i(t) \tag{10}$$

The analytical solution of Eqs. (9) and (10) is determined by ice vertical growing mode as well as the specific structure of the ice layer.

According to our previous research [11, 12], the structure of ice layer and its growing mode are all sensitive to initial thermal condition. When $T_\infty > 269.15$ K, ice grows smoothly in vertical direction and absolute solid ice layer forms from bottom to up. When $T_\infty < 268.15$ K, ice vertical growing is more complex, which is further divided in two sub-progression: spongy-ice growing and "filling of the spongy ice". The difference in structure and growing mode is contribute to the thermal stability of the interface between substrate and supercooled water [13]. Correspondingly, temperature field should be solved in accord with them respectively.

Dynamic temperature field of simple ice layer

When initial temperature $T_\infty > 269.15$ K, structure of the simple ice layer and temperature filed are shown in Fig. 8a, b.

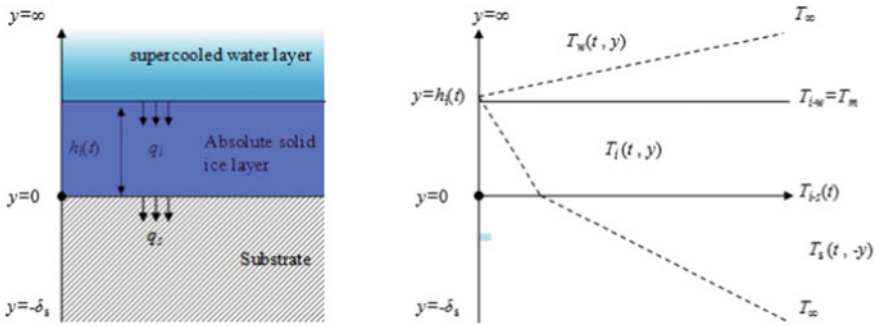

(a) Structure **(b) temperature field**

Fig. 8 Structure and temperature field of simple ice layer $T_\infty > 269.15$ K

As shown in Fig. 8a, as soon as ice being triggered, phase transition occurs smoothly from bottom to up and the latent heat due releases from substrate. In this situation, ice layer grows as an absolutely solid media, in which the temperature field of the on growing ice layer is linearly continuous as shown in Fig. 8b. To derive the analytical solution of transient local temperature of ice layer, three variables $T_{i-w}(t)$, $T_{i-s}(t)$ and *hi(t)* need be identified.

The boundary temperature $T_{i-w}(t)$ is always numerically equal to the equivalent freezing point T_m due to its status of water–ice existence.

$$T_{i-w} \equiv T_m \tag{11}$$

The transient thickness of the layer *hi(t)* at given time t is derived by Eq. (12), which is positive proportional to the square root of time variable t.

$$h_i(t) = 2\eta_i \sqrt{a_i t} \tag{12}$$

In which, η_i is "moving boundary coefficient", which could be derived by the "Stefan approximate solution", as expressed in Eqs. (13) and (14).

$$\eta\sqrt{\pi} = \frac{St_i}{\exp(\eta^2) erf(\eta)} + \frac{St_w}{v \exp(v^2\eta^2) erfc(v\eta)} \tag{13}$$

$$St_i = \frac{c_i \cdot \Delta T_\infty}{L_i} \quad St_w = \frac{c_w \Delta T_\infty}{L_i} \quad v = \sqrt{\frac{a_w}{a_i}} \tag{14}$$

St_i and St_w are the "Stefan number" of ice and supercooled water respectively. In which c_i, c_w are the specific heat capacity of ice and water while a_i, a_w are their heat-diffusion rate. Beside, L_i is the latent heat of ice.

The other boundary temperature $T_{i-s}(t)$ is related to the heat conductivity of the substrate. Since both ice and substrate are solid media at the moment, the heat

conduction and internal temperature field could be described by "multi-wall heat conduction model" [14]. Assume that $T_{i-w}(t)$ at $y = hi(t)$ is T_m and the temperature at the bottom boundary of substrate $y = -\delta_s$ remains at T_∞ constantly. Thus, the boundary temperature at ice-substrate interface could be expressed as Eqs. (15) and (16).

$$T_{i-s}(t) = T_\infty - q\prime(t)\frac{\delta_s}{\lambda_s} \tag{15}$$

$$q\prime(t) = \frac{T_\infty - T_m}{\frac{\delta_s}{\lambda_s} + \frac{h_i(t)}{\lambda_i}} \tag{16}$$

In which $q'(t)$ is the heat flux during heat transfer throughout the "multi-wall" composed of substrate and ice. λ_s, λ_i are the heat transfer coefficient of substrate and ice respectively. Hence, the boundary condition of $T_{i-s}(t)$ is obtained by substituting Eq. (15) into Eq. (16), as shown in Eq. (17).

$$T_{i-s}(t) = T_\infty - \frac{\delta_s \lambda_i (T_\infty - T_m)}{\lambda_i \delta_s + \lambda_s h_i(t)} \tag{17}$$

Above all, since the two boundary condition temperature, $T_{i-s}(t)$,$T_{i-w}(t)$,and the "moving boundary" *hi(t)* are all identified, the temperature field within the on growing ice layer is then expressed by Eq. (17).

$$T_i(t, y) = \frac{T_{i-s}(t) - T_m}{h(t)} \cdot y \tag{18}$$

With such equation, transient local temperature within ice layer is able to be estimated with given freezing time t and position y.

Dynamic temperature field of complex ice layer

When initial temperature $T_\infty < 268.15$ K, structure of "complex" ice layer and temperature filed are shown in Fig. 9a, b.

As shown in Fig. 9a, the structure of ice layer is much complicated than the condition of lower initial temperature. Ice layer could be further divided into three sub-component: as ice crystal layer, spongy ice layer and solid ice layer.

As soon as being triggered, ice crystal grows immediately from substrate towards the water field. Afterward, these ice crystal develops with a plenty of side branches and then links with each other so as to construct spongy ice. Spongy ice is the ice network, which still contains unfrozen liquid component. In following period, freezing of residual liquid component occurs to fill the "cave" of spongy ice and transit it to absolute solid ice layer from bottom to up. The consequential growing of different part construct a complex ice layer. Corresponding to its complex construction, the temperature field could also be divided into three section as shown in Fig. 9b. The

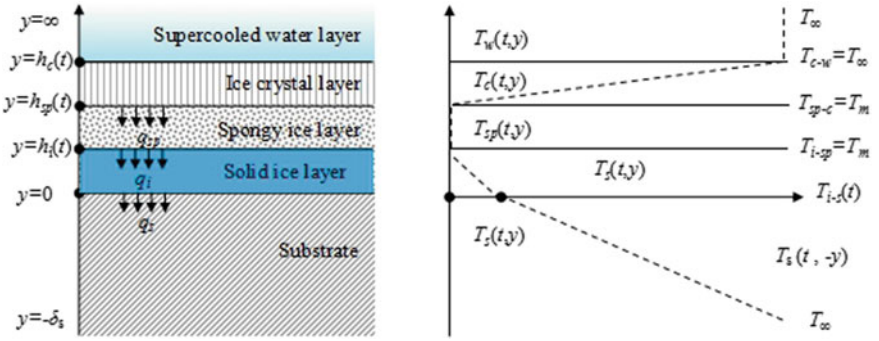

(a) Structure **(b) temperature field**

Fig. 9 Structure and temperature field of "multiple" ice layer $T_\infty < 268.15$ K

analytical solution of temperature $T_i(t, y)$ of each section are expressed in following section.

Temperature field of bottom solid ice layer

As shown in Eq. (18, 19), within the absolute ice layer at bottom, temperature changes linearly, which is similar to that in simple ice vertical growing. The two boundary condition temperature is derived similarly to that of simple ice layer.

$$\begin{cases} T_i(t, y) = \frac{T_{i-s}(t) - T_{i-w}}{h\prime_i(t)} \cdot y \qquad 0 < y < h\prime_i(t) \\ T_{i-w} \equiv T_m \\ T_{i-s}(t) = T_\infty - \frac{\delta_s \lambda_i (T_\infty - T_m)}{\lambda_i \delta_s + \lambda_s h\prime_i(t)} \end{cases} \tag{19}$$

While the analytical solution for moving boundary layer of bottom solid layer is somewhat different to that of simple ice layer.

$$\begin{cases} h\prime_i(t) = 2\eta\prime_i \sqrt{a_i t} \\ \eta\prime_i = \sqrt{\frac{(T_m - T_\infty)c_i}{2 \cdot L\prime_i}} = \sqrt{\frac{(T_m - T_\infty)c_i}{2 \cdot (1 - f) \cdot L_i}} \end{cases} \tag{20}$$

In which, L_i'is the latent heat released by the freezing of those residual liquid component, where f is the dimensionless solid component fraction of the spongy ice. According to Makkonen [15], f is negatively relate to initial temperature. For $T_\infty > 273.15 - 263.15$ K, $f \approx 0.56$–0.7.

Temperature field of bottom solid ice layer

As shown in Eq. (21), within the range of spongy ice layer, temperature is constantly numerically equal to equilibrium freezing point T_m due to the status of ice-water coexistence.

$$T_{sp}(t, y) \equiv T_m \quad h\prime_i(t) \le y \le h_{sp}(t) \tag{21}$$

The moving boundary of spongy ice $h_{sp}(t)$ could also be derived by "Stefan approximate solution". However, the difference is that the thermal-physical properties of spongy ice-layer should be used to replace that of absolute solid ice layer with solid fraction f as expressed in Eq. (22).

$$\begin{cases} T_{sp}(t, y) \equiv T_m \quad h\prime_i(t) \le y \le h_{sp}(t) \\ h_{sp}(t) \approx \sqrt{\frac{|T_m - T_\infty| \cdot c_{sp}}{2 f L_i}} \sqrt{4 a_{sp} t} \end{cases} \tag{22}$$

c_{sp}, a_{sp} and λ_{sp} are the specific heat, heat diffusion coefficient and heat conductivity of spongy ice. They are calculated by consideration the solid fraction f as well as corresponding thermal-physical properties of water and ice respectively as shown Eqs. (23a)–(23c).

$$c_{sp} = f \times c_i + (1 - f) \times c_w \tag{23a}$$

$$\frac{1}{\lambda_{sp}} = \frac{f}{\lambda_i} \times + \frac{1 - f}{\lambda_w} \tag{23b}$$

$$\begin{cases} \rho_{sp} = f \cdot \rho_i \\ a_{sp} = \frac{\lambda_{sp}}{c_{sp} \cdot \rho_{sp}} \end{cases} \tag{23c}$$

By piecewise function of Eqs. (18)–(23a, 23b, 23c), the temperature field of such complex on growing ice layer is also analytically solved.

5 Model for Ice Adhesion/Cohesion Evolution

In Sect. 4.2, the variation of temperature fields of both solid ice layer during its simple vertical growing and complex ice layer during its composite vertical growing are both identified by analytical solution. Since the temperature is the important factor for both ice adhesion and cohesion, their evolution during substrate-icing progression could be modeled based on temperature variation.

5.1 Model of Ice Adhesion Evolution

Ice adhesive strength τ_{ad} is regarded as the function of freezing temperature in most of the researches. Guerin's [6] result of steady static adhesion is quoted as the reference for establishing the relationship between initial temperature and adhesive stress.

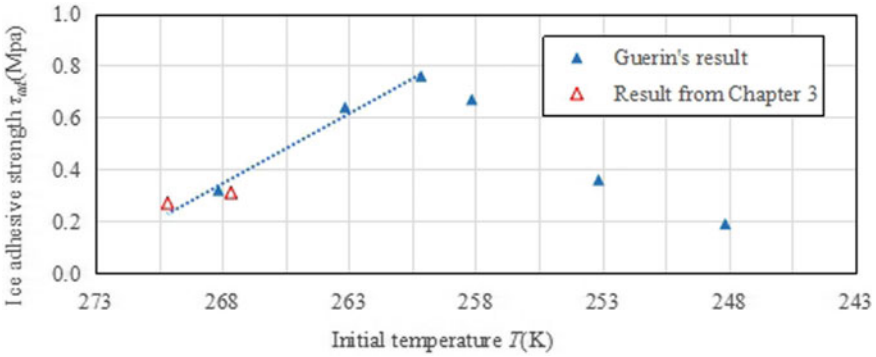

Fig. 10 Relationship between temperature and steady static ice adhesive strength

As shown in Fig. 10, steady static τ_{ad} is negatively proportional to initial temperature within the interval of [273.15, 261.15 K] while it turns positively proportional in the interval of [261.15, 248.15 K]. By linear data fitting, the relationship between τ_{ad} and T within the interval [261.15, 273.15 K] is best expressed by Eq. (24).

$$\tau_{ad}(T_\infty) = 0.612 \times |T_\infty - 273.15\,\mathrm{K}| \quad T_\infty \in [261.15\,\mathrm{K}, 273.15\,\mathrm{K}] \tag{24}$$

In the equation above, temperature is regarded as constant. However, as discussed in Chap. "Analysis of Supersonic Axisymmetric Air Intake in Off-Design Mode", temperature at substrate-ice layer interface changes over time. Therefore, τ_{ad} accordingly turns to a time-dependent variable $\tau_{ad}(t)$ with given initial temperature T_∞. The evolutionary law of $\tau_{ad}(t)$ is expressed as Eq. (25).

$$\tau_{ad}(t) = 0.612 \times \left| T_\infty - \frac{\delta_s \lambda_i (T_\infty - T_m)}{\lambda_i \delta_s + \lambda_s h_i(t)} - 273.15\,\mathrm{K} \right| \tag{25}$$

In Eq. (25), λ_s, λ_i, c_i, L_i, a_i are the constant of physical or thermal properties of substrate and ice, while *hi(t)* refer to Eqs. (12)–(14).

5.2 Model of Ice Adhesion Evolution

Referring to the early result of Han [16], ice cohesive strength τ_{co} is expressed as the power function of the relative temperature ΔT as shown in Eq. (26).

$$[\tau_{co}] = 0.258 \times |\Delta T|^{0.78} \quad |\Delta T| \in [0\,\mathrm{K}, 30\,\mathrm{K}] \tag{26}$$

Table 5 Ice cohesion within different temperature in relevant literature

$\|\Delta T\|$ (K)	≈0	2	5	10
τ_{co}(Mpa)	≈0.28	≈0.31	0.34	0.35

According to Bernard's induction, however, ice cohesion is null at freezing point T_m, which is not reasonable in reality. Therefore, an intercept, $\tau_{co}(\Delta T = 0)$, at freezing point is necessary to create a more comprehensive description.

To obtain the corrected equation for "$T-\tau_{co}$" relationship, "indefinite coefficient algorithm" is used by carrying over the power function as shown in Eq. (27) and then referring to a series of discrete results of τ_{co} (ΔT) as shown in Table 5 [17].

$$[\tau_{co}] = b_0 + b_n|\Delta T|^n \tag{27}$$

The corrected equation is shown in Eq. (28), which represents the relationship between static ice cohesive strength and temperature.

$$\tau_{co}(\Delta T) = \tau_{co}(\Delta T = 0) + b|\Delta T|^n = 0.28 + 0.0219|\Delta T|^{0.5385} \tag{28}$$

In Sect. 4, the temperature is expressed with both variable for time t and position y during the progression of ice vertical growing. Thus, evolution of ice cohesive strength is identified by using temperature variation as the "transfer function".

For those growing of absolute solid ice layer when $T_\infty < 269.15\,\mathrm{K}$, τ_{co} is expressed as Eq. (29). In which the transient local temperature of the ice layer refers to Eq. (17).

$$\tau_{co}(t) = \begin{cases} 0.28 + 0.0219|T_i(t, y) - T_m|^{0.5385} & 0 < y < h_i(t) \\ 0 & y > h_i(t) \end{cases} \tag{29}$$

Here *hi(t)* and $T_i(t, y)$ refer to Eqs. (12) and (19). Within the range of the transient solid ice layer, the evolution of τ_{co} could be roughly estimated by corresponding time t and position y.

For those growing of complex ice layer with lower initial temperature, τ_{co} is expressed as Eq. (30).

$$\tau_{co}(t) = \begin{cases} 0.28 + 0.0219|T_i(t, y) - T_m|^{0.5385} & 0 < y < h\prime_i(t) \\ f \cdot \tau_{co}[\Delta T = 0] = 0.7 \times 0.28 \approx 0.2 & h\prime_i(t) < y < h_{sp}(t) \\ 0 & y > h_{sp}(t) \end{cases} \tag{30}$$

Evaluation of τ_{co} is more complicated for complex ice layer. The transient range of solid ice layer *hi'*(t) and spongy ice layer $h_{sp}(t)$ should be calculated with the given t to identify whether the given position y is in the solid ice layer or spongy ice layer. Therefore, the evolution of τ_{co} could be evaluated by corresponding part of the piece-wise functions as expressed in Eq. (30).

Here $h'_i(t)$, $h_{sp}(t)$ and $T_i(t, y)$ refer to Eqs. (18), (19), (20) and (22) Within the range of solid ice layer, τ_{co} is power functional with the evolutionary local temperature $T(t, y)$. Within the range of spongy ice layer, τ_{co} is constant equal to the ice cohesive strength at equilibrium freezing point, which consider the effect of solid fraction.

6 Conclusion

In this paper, the evolutionary principle of both adhesive strength τ_{ad} and cohesive strength τ_{co} during substrate icing are validated experimentally and analyzed theoretically. Evolution due to both physical properties as well as thermal condition are presented. The following conclusions are drawn:

(1) Ice adhesion and cohesion are two totally different ice mechanical performance, which could not be replaced by each other.
(2) In the condition with a constant initial temperature, both ice adhesion and cohesion increase obviously with freezing time especially at the early stage of substrate-icing progression and then become convergent in the end.
(3) The evolutionary trend of both ice adhesion and cohesion are strongly relate to the temperature variation of the ice layer, which is determined by their structure of as well as their growing pattern.
(4) A model expressed by piece-wise functions is established to predict the evolutionary of ice adhesion and cohesion in both temporal and spatial. By this model, adhesive strength and cohesive strength could be quickly estimated with given variables of initial temperature, time and position.

Acknowledgements The project is not supported by any Foundation.

References

1. Chen G, Yang K, Wang LP et al (2018) Test of ice shedding on turbofan engine blade in refrigeratory environment. J Beijing Univ Aeronaut Astronaut 44(010):2106–2114
2. Kraj AG, Bibeau EL (2010) Measurement method and results of ice adhesion force on the curved surface of a wind turbine blade. Renew Energy 35:741–746
3. Zou M, Beckford S, Wei R et al (2011) Effects of surface roughness and energy on ice adhesion strength. Appl Surf Sci 257:3786–3792
4. Kulinich SA, Farzaneh M (2009) Ice adhesion on super-hydrophobic surfaces. Appl Surf Sci 255:8153–8157
5. Jellinek HHG (1962) Ice adhesion. Can J Phys 40(10):1294–1309
6. Guerin F, Laforte C, Farinas MI et al (2016) Analytical model based on experimental data of centrifuge ice adhesion tests with different substrates. Cold Reg Sci Technol 121:93–99
7. Janjua ZA (2017) The influence of freezing and ambient temperature on the adhesion strength of ice. Cold Reg Sci Technol 140:14–19

8. Archer P, Gupta V (1999) Measurement and control of ice adhesion to aluminum 6061 alloy. J Mech Phys Solids 46(10):1745–1771
9. Scavuzzo RJ, Chu ML, Kellackey CJ (1996) Impact ice stresses in rotating airfoils. J Aircr 28(7):450–455
10. Liu Z, Kong WL, Liu H (2018) Experimental study for effect of mean volumetric diameter on ice adhesion strength. J Exp Fluid Mechan 32:35–39
11. Kong WL, Liu H (2018) Unified icing theory based on phase transition of supercooled water on a substrate. Int J Heat Mass Transf 123:896–910
12. Chen G, Kong WL, Wang LP, Wang FX (2020) On the experimental and theoretical model for ice crystal characteristics near a substrate. Int J Heat Mass Transf 152:119462
13. Kong WL (2015) Mechanism and fundamental theory of supercooled water solidification on the abnormal aircraft icing. Dissertation, Shanghai Jiao Tong university
14. Tao WQ (2018) Heat transfer. Higher Education Press, Beijing
15. Makkonen L (2010) Solid fraction in dendritic solidification of a liquid. Appl Phys Lett 96:091910
16. Bernard M (1978) The strength of polycrystalline ice. Can J Civ Eng 5(3):285–300
17. Jia Q, Li ZJ (2015) Experimental study on shear strength of freshwater Ice in a Reservoir. Math Pract Theory 45(5):132–137
18. Tirmizi SH, Gill WN (1987) Effect of natural convection on growth velocity and morphology of dendritic ice crystals. J Cryst Growth 85:488–502